Proceedings of COBEM 2007
19th International Congress of Mechanical Engineering
November 5-9, 2007, Brasília, DF

THE SINGULAR BEHAVIOR OF A ROTATING DISK UNDER EXTERNAL PRESSURE

Adair R. Aguiar, aguiarar@sc.usp.br
William C. Silva, wcsilva@eesc.usp.br
Department of Structural Engineering, University of São Paulo, 13560-590, São Carlos, SP

Abstract. *This work represents a contribution to the understanding of singular problems in anisotropic elasticity. It concerns the solution of the rotationally symmetric disk problem in the context of both the classical linear theory and a constrained theory that prevents self-intersection to occur. The problem concerns the rotation of a homogeneous and cylindrically anisotropic circular disk about its center with a constant angular velocity. The disk is radially compressed along its external contour by a uniformly distributed normal traction. The case of zero angular velocity has been treated elsewhere. In the linear theory, it is shown that there exists a region within the disk where self-intersection occurs for any value of the compressive external force and for a certain range of material parameters. In addition, strains are unbounded at the center of the disk. In the constrained theory, the self-intersecting behavior is eliminated. For the rotating disk, it is shown that no self-intersection occurs for values of the compressive force that are small compared to the square of the angular velocity. In fact, if a certain relation between this force and the angular velocity is attained, the strains are bounded everywhere. For other values of the compressive force, the self-intersecting behavior is still observed in the linear theory and is eliminated in the context of the constrained theory.*

Keywords: *Elasticity, Cylindrical Anisotropy, Constrained Optimization, Singularity, Self-intersection*

1. INTRODUCTION

Strain singularities in Classical Linear Elasticity contradict the very basic assumption of the theory, which is that strains should be infinitesimal. If the strains become large in the vicinity of a point in the body, then nonlinear effects should be taken into account in the analysis of the material behavior in this vicinity. Strain singularities are also related to physically unrealistic behavior, such as material overlapping (see, for instance, Aguiar (2001) and references cited therein). Nevertheless, the theory can still be used to predict the material behavior in regions where the strains are infinitesimal.

In this work, we use the constrained minimization theory of Fosdick & Royer-Carfagni (2001) to study a particular class of problems in Classical Linear Elasticity for which material overlapping can occur inside the body. We are particularly interested in the uniform radial compression of a circular disk of radius ρ_e that is rotating with a constant angular velocity ω about its center. The disk is homogeneous and cylindrically anisotropic.

The case of zero angular velocity has been treated by Fosdick & Royer-Carfagni (2001). In the linear theory, it is shown that there exists a region within the disk where self-intersection occurs for any value of the compressive external force p and for a certain range of material parameters. In addition, strains are unbounded at the center of the disk. In the constrained theory, the self-intersecting behavior is eliminated by considering two non-intersecting regions inside the disk: A central core of radius ρ_a where the determinant of the deformation field, J, is equal to a small parameter $\varepsilon > 0$ and an annulus of inner radius ρ_a and outer radius ρ_e where $J \geq \varepsilon$. The radius ρ_a is the unique solution of an algebraic equation obtained from the imposition of boundary conditions. As the pressure p increases, ρ_a increases, reaching the value of ρ_e for a certain critical value of p. Beyond this critical value, the whole region occupied by the disk is such that $J = \varepsilon$.

For the rotating disk, we show in Section 2 that, in the context of the classical linear theory, no self-intersection occurs for values of p that are small compared to ω^2. In fact, if a certain relation between p and ω is attained, the strains are bounded everywhere. For other values of p, the self-intersecting behavior is still observed in the linear theory for the same range of material parameters considered by Fosdick & Royer-Carfagni (2001). We then show in Section 3 that the overlapping can be eliminated in the context of the constrained theory. For small enough p and ω, we have two non-intersecting regions coexisting inside the disk: A central core of radius ρ_a where $J = \varepsilon$ and an annulus with inner radius ρ_a and outer radius ρ_e where $J \geq \varepsilon$. Here, too, ρ_a is the unique solution of an algebraic equation in the interval $[0, \rho_e]$. As both p and ω reach certain critical values, however, the algebraic equation may admit two, one, or, no roots in the interval $(0, \rho_e)$. We use this fact to investigate the possibility of the disk to support not two, but three non-intersecting regions: A central core of radius ρ_a where $J = \varepsilon$, an annulus with inner radius ρ_a and outer radius ρ_b where $J \geq \varepsilon$, and an annulus with inner radius ρ_b and outer radius ρ_e where $J = \varepsilon$. In Section 4 we present numerical results obtained from analytical and computational investigations that show the existence of such regions.

2. THE UNCONSTRAINED DISK PROBLEM

Lekhnitskii (1968) considers the equilibrium of a circular homogeneous disk of external radius ρ_e, which is radially compressed along its external contour by a uniformly distributed normal force p per unit length. He also considers the equilibrium of a rotating circular homogeneous disk with angular velocity ω. In both cases, the disk is linearly elastic and cylindrically aeolotropic. In this work, we consider that the disk is both rotating at the constant angular velocity ω and being radially compressed by the normal force p. Depending on the values of ω and p, the solution of this problem predicts material overlapping.

The problem is two-dimensional so that, relative to the usual orthonormal cylindrical basis $(\mathbf{e}_\rho, \mathbf{e}_\theta)$, the stress and strain tensors are given by

$$\mathbf{T} = \sigma_{\rho\,\rho}\,\mathbf{e}_\rho \otimes \mathbf{e}_\rho + \sigma_{\theta\,\theta}\,\mathbf{e}_\theta \otimes \mathbf{e}_\theta + \sigma_{\rho\,\theta}\,(\mathbf{e}_\rho \otimes \mathbf{e}_\theta + \mathbf{e}_\theta \otimes \mathbf{e}_\rho)\,, \tag{1}$$

$$\mathbf{E} = \epsilon_{\rho\,\rho}\,\mathbf{e}_\rho \otimes \mathbf{e}_\rho + \epsilon_{\theta\,\theta}\,\mathbf{e}_\theta \otimes \mathbf{e}_\theta + \epsilon_{\rho\,\theta}\,(\mathbf{e}_\rho \otimes \mathbf{e}_\theta + \mathbf{e}_\theta \otimes \mathbf{e}_\rho)\,, \tag{2}$$

respectively. These tensors are related to each other by the linear constitutive relations

$$\sigma_{\rho\,\rho} = \frac{1}{1-\nu_\rho\nu_\theta}(E_\rho\,\epsilon_{\rho\rho} + \nu_\rho\,E_\theta\,\epsilon_{\theta\theta})\,, \qquad \sigma_{\theta\,\theta} = \frac{1}{1-\nu_\rho\nu_\theta}(\nu_\theta\,E_\rho\,\epsilon_{\rho\rho} + E_\theta\,\epsilon_{\theta\theta})\,, \qquad \sigma_{\rho\,\theta} = 2\,G\,\epsilon_{\rho\theta}\,, \tag{3}$$

where $E_\rho, E_\theta, \nu_\rho, \nu_\theta$, and G are elastic constants that satisfy

$$\frac{\nu_\rho}{E_\rho} = \frac{\nu_\theta}{E_\theta}\,, \quad E_\rho > 0\,, \quad E_\theta > 0\,, \quad G > 0, \quad (1-\nu_\rho\,\nu_\theta) > 0\,. \tag{4}$$

Since uniqueness is guaranteed in classical linear elasticity, the displacement field must be rotationally symmetric with respect to the center of the disk, i.e., $\mathbf{u}(\rho,\theta) = u(\rho)\,\mathbf{e}_\rho$. Thus, the strain components take the form

$$\epsilon_{\rho\rho} = u'\,, \qquad \epsilon_{\theta\theta} = \frac{u}{\rho}\,, \qquad \epsilon_{\rho\theta} = 0\,, \tag{5}$$

where $(\cdot)' \equiv d\,(\cdot)/d\,\rho$. Also, the disk is rotating with a constant angular velocity ω[1]. In the absence of body force, the only non-trivial equilibrium equation is given by

$$\frac{\partial\sigma_{\rho\rho}}{\partial\rho} + \frac{\sigma_{\rho\rho}-\sigma_{\theta\theta}}{\rho} + \gamma\,\omega^2\,\rho = 0\,, \tag{6}$$

where γ is the mass per unit volume of the material of the disk.

Because of (1)-(5), the equation (6) becomes

$$u'' + \frac{u'}{\rho} - \kappa^2\,\frac{u}{\rho^2} + \hat{\omega}\,\rho = 0\,, \tag{7}$$

where

$$\kappa \equiv \sqrt{\frac{E_\theta}{E_\rho}} > 0\,, \qquad \hat{\omega} \equiv \frac{\gamma\,\omega^2\,(1-\nu_\rho\nu_\theta)}{E_\rho}\,. \tag{8}$$

The solution of the ordinary differential equation (7) that satisfies the kinematic condition $u(0) = 0$ and the pressure condition on the outer radius, $\sigma_{\rho\rho}(\rho_e) = -p$, is given by

$$u(\rho) = \alpha_1\,\rho^{\,\kappa} - \alpha_2\,\rho^3\,, \tag{9}$$

where

$$\begin{aligned} \alpha_1 &= \frac{\rho_e^{-\kappa+1}\,\left[-\hat{p} + \hat{\omega}\,\rho_e^2\,(3+\nu_\theta)/(9-\kappa^2)\right]}{\kappa+\nu_\theta}\,, \qquad \alpha_2 = \frac{\hat{\omega}}{9-\kappa^2}\,, \qquad \text{if } \kappa \neq 3\,, \\ \alpha_1 &= \frac{-\hat{p} + \hat{\omega}\,\rho_e^2/6}{\rho_e^2\,(3+\nu_\theta)}\,, \qquad \alpha_2 = \frac{\hat{\omega}}{6}\,, \qquad \text{if } \kappa = 3\,. \end{aligned} \tag{10}$$

In (10),

$$\hat{p} \equiv \frac{1-\nu_\rho\,\nu_\theta}{E_\rho}\,p\,. \tag{11}$$

[1] The case $\hat{\omega} = 0$ is treated by Fosdick & Royer-Carfagni (2001).

Notice from both the inequality (4.e) and the definition of κ in (8) together with (4.a) that both inequalities $\kappa + \nu_\theta > 0$ and $\kappa - \nu_\theta > 0$ hold for $\kappa > 0$.

The deformation associated with the displacement field $\mathbf{u}(\rho, \theta) = u(\rho)\,\mathbf{e}_\rho$ is given by $\mathbf{f}(\rho, \theta) = [\rho + u(\rho)]\,\mathbf{e}_\rho$ and its Jacobian determinant $J \equiv \det \nabla\mathbf{f}$ is given by

$$J = \varphi_\rho\,\varphi_\theta\,, \qquad \varphi_\rho = 1 + u'\,, \qquad \varphi_\theta = 1 + \frac{u}{\rho}\,. \tag{12}$$

In (12), φ_ρ and φ_θ are the principal stretches at a point $\mathbf{x} = \rho\,\mathbf{e}_\rho$ along the radial and tangential directions, respectively.

To interpret these measures of deformation physically, we consider that $\mathbf{x}$ is at the center of a sector of the disk, as illustrated in Fig. 1. In its reference configuration, the sector has radial length $d\,\rho$ and angle $d\,\theta$. After deformation, $d\,\rho$ becomes $\varphi_\rho\,d\,\rho$ and an arc of length $\rho\,d\,\theta$ passing through $\mathbf{x}$ becomes $\rho\,\varphi_\theta\,d\,\theta$. Since an element of area does not vanish in any continuous process starting in the reference configuration[2], we must have both $\varphi_\rho > 0$ and $\varphi_\theta > 0$ for $\rho > 0$, which implies that $J > 0$ from (12). The converse is not true, that is, a deformation with $J > 0$ may not be reached by a continuous process starting in the reference configuration since we may have both $\varphi_\rho < 0$ and $\varphi_\theta < 0$.

Next, we analyze the conditions under which either $\varphi_\rho \le 0$ or $\varphi_\theta \le 0$. To avoid the outer surface of the disk to be crushed into a single point at its center, we assume that $-u(\rho_e)/\rho_e < 1$, which can be rewritten as $\varphi_\theta(\rho_e) > 0$ by means of (12.c). We then see from (9) together with (8.b), (10), and (11) that this inequality imposes a restriction on the values of $\hat{p}$ and $\hat{\omega}$ according to the expression

$$\hat{p} < \hat{p}_\theta \equiv \kappa + \nu_\theta + \frac{\hat{\omega}\,\rho_e^2}{3 + \kappa} \qquad \text{for} \quad \kappa > 0\,. \tag{13}$$

We shall assume this restriction throughout this section.

If $\kappa \ge 1$, it follows from (12.c) together with (9) and (10) that $\varphi_\theta(\rho) > 0$ for $\rho \in [0, \rho_e]$.

If $\kappa < 1$, the behavior of φ_θ is dictated by the sign of α_1 in (10.a), which in turn depends on the values of $\hat{p}$ and $\hat{\omega}$. If $\hat{p} < \hat{q}$, where $\hat{q}$ is given by

$$\hat{q} = \hat{\omega}\,\rho_e^2\,(3 + \nu_\theta)/(9 - \kappa^2)\,, \tag{14}$$

then $\alpha_1 > 0$ and it follows from (12.c) together with (9) and (10.a) that $\varphi_\theta(\rho) \to \infty$ as $\rho \to 0$. Also,

$$\varphi_\theta'(\rho) = \alpha_1\,(\kappa - 1)\,\rho^{\kappa - 2} - \frac{2\,\hat{\omega}\,\rho}{9 - \kappa^2} \tag{15}$$

is negative in $(0, \rho_e)$. Since $\varphi_\theta(\rho_e) > 0$, $\varphi_\theta(\rho)$ is positive and strictly decreasing in $(0, \rho_e)$.

On the other hand, if $\hat{p} \ge \hat{q}$, where $\hat{q}$ is given by (14), then $\alpha_1 \le 0$ and it follows from the inequality (13) that $\hat{\omega} < (9 - \kappa^2)/\rho_e^2$. If $\alpha_1 = 0$, then $\varphi_\theta(\rho) = 1 - \hat{\omega}\,\rho^2/(9 - \kappa^2) > 1 - (\rho/\rho_e)^2 > 0$ since $\rho \in (0, \rho_e)$. If $\alpha_1 < 0$, there exists a unique root $\hat{\rho} \in (0, \rho_e)$ of the algebraic equation $\varphi_\theta(\rho) = 0$. To see this, observe from (12.c) together with (9) and (10.a) that $\varphi_\theta(\rho) \to -\infty$ as $\rho \to 0$. Moreover, we see from (15) that $\varphi_\theta''(\rho) < 0$ for $\rho \in (0, \rho_e)$. Therefore, $\varphi_\theta(\rho)$ is a concave function of ρ that is negative near the center of the disk and positive at $\rho = \rho_e$. The conclusion then follows.

Next, we analyze the conditions under which $\varphi_\rho \le 0$. For this, it follows from (12.b) together with (9) that

$$\begin{aligned} \varphi_\rho(\rho) &= \alpha_1\,\kappa\,\rho^{\kappa - 1} - 3\,\hat{\omega}\,\rho^2/(9 - \kappa^2) + 1 \qquad \text{for} \quad \kappa \ne 3\,, \\ \varphi_\rho(\rho) &= (3\,\alpha_1 - \hat{\omega}/2)\,\rho^2 + 1 \qquad \text{for} \quad \kappa = 3\,, \end{aligned} \tag{16}$$

respectively, where $\hat{\omega}$ is given by (8.b) and α_1 is given by (10.a) for $\kappa \ne 3$ and by (10.b) for $\kappa = 3$. Observe from (16) that, at $\rho = 0$, φ_ρ is unbounded for $\kappa < 1$, equals to $\alpha_1\,\kappa + 1$ for $\kappa = 1$, and is one for $\kappa > 1$.

If $\kappa < 1$, we have two cases depending on the sign of α_1 in (10.a), which in turn depends on the values of $\hat{p}$ and $\hat{\omega}$. If $\hat{p} \le \hat{q}$, where $\hat{q}$ is given by (14), then $\alpha_1 \ge 0$ and it follows from (16) that $\varphi_\rho(\rho)$ is a monotonically decreasing function of ρ, which reaches its minimum at $\rho = \rho_e$. This minimum can be negative for $\hat{p} > \hat{p}_\rho$, where $\hat{p}_\rho$ is given by

$$\hat{p}_\rho \equiv \frac{1}{\kappa}\left[\kappa + \nu_\theta - \frac{\hat{\omega}\,\rho_e^2\,\nu_\theta}{3 + \kappa}\right]\,. \tag{17}$$

For $\hat{q} \ge \hat{p} > \hat{p}_\rho$, it follows from both (14) and (17) that we must have $\hat{\omega} > (9 - \kappa^2)/(3\,\rho_e^2)$. In addition, the inequalities $\hat{p}_\theta \ge \hat{p} > \hat{p}_\rho$, where $\hat{p}_\theta$ is given by (13), yield $\hat{\omega} > (1 - \kappa)\,(3 + \kappa)/\rho_e^2$. Thus, it is possible to find values for both $\hat{p}$ in the range $(\hat{p}_\theta, \hat{p}_\rho)$ and $\hat{\omega} > (9 - \kappa^2)/\rho_e^2$ such that *the local injectivity is lost at a point close to the boundary* $\rho = \rho_e$*, even though the global injectivity is preserved*. Now, notice from (17) that if $\hat{\omega} \approx (\kappa + \nu_\theta)\,(3 + \kappa)/(\nu_\theta\,\rho_e^2)$ for $\nu_\theta > 0$, the value of $\hat{p}_\rho$ would be very small, which in turn would allow to choose a very small value of $\hat{p}$ in the range $(\hat{p}_\rho, \hat{p}_\theta)$. The

[2] By a continuous process starting in the reference configuration, we mean a continuous one-parameter family $\mathbf{f}_\sigma$ $(0 \le \sigma \le 1)$ of deformations with $\mathbf{f}_0 = \mathbf{x}$, $\mathbf{f}_1 = \mathbf{f}$, and $\det \nabla\mathbf{f}_\sigma$ never zero (Gurtin, 2001).

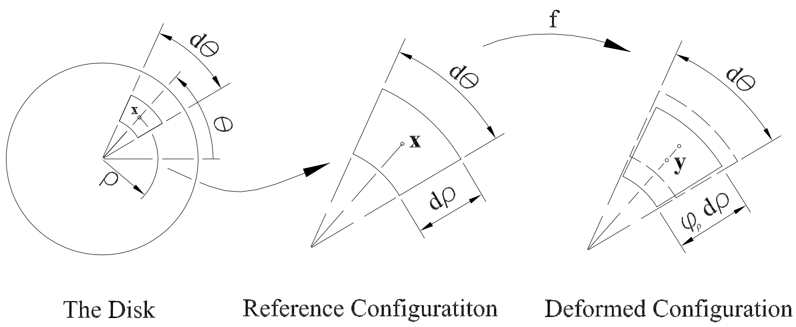

Figure 1. The reference and deformed configurations of a sector of the disk.

corresponding value of ω, given by (8), would have to be, however, very high. Because of these considerations, we shall assume that $\hat{p} < \hat{p}_\rho$, which means that no self-intersection is possible for $\alpha_1 \geq 0$.

Next, consider the case $\hat{p} > \hat{q}$, which corresponds to $\alpha_1 < 0$, and assume that $\hat{p} < \hat{p}_\rho$ to ensure that $\varphi_\rho(\rho_e) > 0$. Then, φ_ρ is a concave function, which is negative at the center of the disk, and therefore has a unique root in the interval $(0, \rho_e)$. A necessary condition to ensure that $\hat{q} < \hat{p} < \hat{p}_\rho$ is obtained from (14) and (17) and is given by $\hat{\omega} < (9 - \kappa^2)/(3\,\rho_e^2)$. This condition also ensures that $\hat{p} < \hat{p}_\theta$, where $\hat{p}_\theta$ is given by (13).

If $\kappa \geq 1$, φ_ρ is bounded at $\rho = 0$ and it is not difficult to show that φ_ρ is positive in $(0, \rho_e)$, provided that $\hat{p}$ is smaller than both $\hat{p}_\theta$, given by (13), and $\hat{p}_\rho$, given by (17).

In summary, in this section we assume that both $\hat{p} < \hat{p}_\theta$ and $\hat{p} < \hat{p}_\rho$. We then find that both φ_θ and φ_ρ are positive in $(0, \rho_e)$ for either $\kappa \geq 1$ or $\kappa < 1$ together with $\hat{p} < \hat{q}$. Thus, the rotating disk has no self-intersecting behavior for compressive forces that are small compared to the square of the angular velocity. On the other hand, if both $\kappa < 1$ and $\hat{p} > \hat{q}$, then both φ_θ and φ_ρ are negative in sub-intervals of $(0, \rho_e)$, characterizing self-intersection in the disk. In particular, both are negative near the center of the disk, yielding $J > 0$ from (12). Thus, $J > 0$ is not sufficient to prevent self-intersection from occurring. To prevent it, we must have both $\varphi_\theta > 0$ and $\varphi_\rho > 0$.

3. THE CONSTRAINED DISK PROBLEM

The solution of the unconstrained disk problem in Section 2 predicts material overlapping for $\kappa \in (0, 1)$. In this section, we consider that $\kappa \in (0, 1)$ and formulate the disk problem as a minimization problem subjected to the constraint that the injectivity must be preserved. We then present first variation conditions for the existence of a minimizer and solve the corresponding equations to determine this minimizer.

Let $\mathcal{B} \subset \mathbb{R}^2$ be the undistorted natural reference configuration of the disk and let

$$\mathcal{A}_\varepsilon \equiv \{\mathbf{v} : \mathcal{W}^{1,2}(\mathcal{B}) \to \mathbb{R}^2 \big| \det(\mathbf{1} + \nabla\mathbf{v}) \geq \varepsilon > 0, \mathbf{v} = \mathbf{0} \text{ on } \rho = 0\} \tag{18}$$

be the class of admissible displacement fields of the form $\mathbf{v}(\rho, \theta) = \vartheta(\rho)\,\mathbf{e}_\rho$, where $\varepsilon > 0$ is sufficiently small and $\mathcal{W}^{1,2}(\mathcal{B})$ is the set of all square integrable functions with square integrable derivatives in $\mathcal{B}$.

We consider the problem of minimum potential energy for the rotating disk[3]:

$$\min_{\mathbf{v} \in \mathcal{A}_\varepsilon} \mathcal{E}[\mathbf{v}]\,, \qquad \mathcal{E}[\mathbf{v}] \equiv \frac{1}{2}\,a[\mathbf{v}, \mathbf{v}] - f[\mathbf{v}]\,, \tag{19}$$

where $\mathcal{A}_\varepsilon$ is given by (18) and

$$a[\mathbf{v}, \mathbf{v}] \equiv \frac{1}{2}\int_0^{\rho_e} \left[(\vartheta')^2 + \kappa^2\,\frac{\vartheta^2}{\rho}\right]\,d\rho + \frac{\nu_\theta}{2}\,\vartheta^2(\rho_e)\,, \qquad f[\mathbf{v}] \equiv \hat{\omega}\int_0^{\rho_e} \vartheta\,\rho^2\,d\rho - \hat{p}\,\vartheta(\rho_e)\,\rho_e\,, \tag{20}$$

with κ, $\hat{\omega}$, and $\hat{p}$ being given by (8.a, b), and (11), respectively. The functional $\mathcal{E}[\cdot]$ times $2\,\pi\,E_\rho/(1 - \nu_\rho\,\nu_\theta)$ is the total potential energy of the cylindrically aeolotropic disk in classical linear elasticity.

We now assume that, for some $\rho_a \in [0, \rho_e]$, $(0, \rho_a)$ and (ρ_a, ρ_e) are sub-intervals of $(0, \rho_e)$ where the constraint of local injectivity is active ($\det\nabla\mathbf{f} = \varepsilon$) and non-active ($\det\nabla\mathbf{f} > \varepsilon$), respectively. First variation conditions for the existence of a minimizer $\mathbf{u}(\rho, \theta) = u(\rho)\,\mathbf{e}_\rho \in \mathcal{A}_\varepsilon$ of (19), (20) are derived by Fosdick & Royer-Carfagni (2001) and are given by

[3]The general statement of the minimization problem, valid for dimensions 2, or, 3, is stated in Fosdick & Royer-Carfagni (2001).

- The Euler-Lagrange equations:

$$\begin{aligned} u'' + \frac{u'}{\rho} - \kappa^2\,\frac{u}{\rho^2} + \hat{\omega}\,\rho - \left(1 + \frac{u}{\rho}\right)\frac{d\,\hat{\lambda}}{d\,\rho} &= 0\,, \qquad \hat{\lambda} \geq 0\,, \qquad \text{for } \rho \in (0, \rho_a)\,, \\ u'' + \frac{u'}{\rho} - \kappa^2\,\frac{u}{\rho^2} + \hat{\omega}\,\rho &= 0 \qquad \text{for } \rho \in (\rho_a, \rho_e)\,. \end{aligned} \tag{21}$$

- The kinematic and boundary conditions:

$$u(0) = 0\,, \qquad u'(\rho) + \nu_\theta\,\frac{u(\rho)}{\rho} = -\hat{p} \qquad \text{for } \rho = \rho_e\,. \tag{22}$$

- The jump conditions across $\rho = \rho_a$:

$$u(\rho_a^+) = u(\rho_a^-)\,, \qquad u'(\rho_a^+) = u'(\rho_a^-) - \left[1 + \frac{u(\rho_a^-)}{\rho_a}\right]\hat{\lambda}(\rho_a^-)\,, \tag{23}$$

where $\rho_a^\pm \equiv \lim_{\tau \to 0}(\rho_a \pm \tau)$ for $\tau > 0$ and $\hat{\lambda}\,E_\rho/(1 - \nu_\rho\,\nu_\theta)$ is the Lagrange multiplier. The condition (23.b) is obtained from $\sigma_{\rho\,\rho}(\rho_a^+) = \sigma_{\rho\,\rho}(\rho_a^-) - [1 + u(\rho_a^-)/\rho_a]\ \hat{\lambda}(\rho_a^-)$ together with (3), (5), and (23.a). Observe from (23.b) that the jump of u' across $\rho = \rho_a$ is zero provided that $\hat{\lambda}(\rho_a^-) = 0$. We show below that this is indeed the case.

The imposition of the injectivity constraint $\det(\mathbf{1}+\nabla\mathbf{u}) = \varepsilon > 0$ in $(0, \rho_a)$ yields the problem of finding $u : (0, \rho_a) \to \mathbb{R}$ that satisfies

$$\frac{1}{2\,\rho}\frac{d}{d\rho}(\rho + u)^2 = \varepsilon \qquad \text{in } (0, \rho_a)\,, \qquad u(0) = 0\,.$$

The solution of this problem is

$$u(\rho) = \left(\sqrt{\varepsilon} - 1\right)\rho \qquad \text{for } \rho \in (0, \rho_a)\,. \tag{24}$$

Substituting the expression (24) in the first Euler-Lagrange equation (21.a), we obtain a first order differential equation for $\hat{\lambda}$. The solution of this equation is given by

$$\hat{\lambda}(\rho) = \frac{1}{\sqrt{\varepsilon}}\left[\frac{\hat{\omega}}{2}\left[\rho^2 - \tilde{\rho}^2\right] - (1 - \kappa^2)\,(1 - \sqrt{\varepsilon})\log\left(\frac{\rho}{\tilde{\rho}}\right)\right]\,, \tag{25}$$

where $\tilde{\rho} \in \mathbb{R}$ is to be determined consistent with $\hat{\lambda}(\tilde{\rho}) \geq 0$ in $(0, \rho_a)$. We show in Appendix A that $u'(\rho_a^+) = u'(\rho_a^-)$ and that $\tilde{\rho} = \rho_a$, yielding $\hat{\lambda}(\rho_a^-) = 0$.

The general solution of the ordinary differential equation (21.b) is of the form

$$u(\rho) = \alpha^+\,\rho^\kappa + \alpha^-\,\rho^{-\kappa} - \frac{\hat{\omega}}{9 - \kappa^2}\,\rho^3 \qquad \text{for } 0 < \kappa < 1\,, \tag{26}$$

where both constants α^+ and α^- are determined from the jump conditions (23) together with both $\hat{\lambda}(\rho_a) = 0$ from (25) and $\tilde{\rho} = \rho_a$. These constants are given by

$$\alpha^+ = \frac{\rho_a^{-\kappa+1}}{2\,\kappa}\left[-(1 + \kappa)\,(1 - \sqrt{\varepsilon}) + \frac{\hat{\omega}\,\rho_a^2}{3 - \kappa}\right]\,, \qquad \alpha^- = \frac{\rho_a^{\kappa+1}}{2\,\kappa}\left[(1 - \kappa)\,(1 - \sqrt{\varepsilon}) - \frac{\hat{\omega}\,\rho_a^2}{3 + \kappa}\right]\,. \tag{27}$$

We still need to find ρ_a in (27). For this, we substitute (26) together with (27) in the traction condition (22.b) to obtain the algebraic equation

$$0 = r(\zeta) \equiv s(\zeta;\kappa) + s(\zeta;-\kappa) + \hat{p} - \left(\frac{3 + \nu_\theta}{9 - \kappa^2}\right)\hat{\omega}\,\rho_e^2\,, \qquad \zeta \equiv \frac{\rho_a}{\rho_e}\,, \tag{28}$$

where

$$s(\zeta;\kappa) \equiv \left(\frac{\kappa + \nu_\theta}{2\,\kappa}\right)\zeta^{1-\kappa}\left[-(1 + \kappa)\,(1 - \sqrt{\varepsilon}) + \frac{\hat{\omega}\,\rho_e^2}{3 - \kappa}\,\zeta^{\,2}\right] \tag{29}$$

is a function of ζ parameterized by κ.

First, notice from (28) together with (29) that $r(0) = \hat{p} - \hat{q}$, where $\hat{q}$ is given by (14), and that $r(1) = \hat{p} - \hat{p}_0$, where

$$\hat{p}_0 = (1 + \nu_\theta)\,(1 - \sqrt{\varepsilon}) \tag{30}$$

is positive for $\varepsilon > 0$ sufficiently small. Taking the derivative of r, we obtain

$$r'(\zeta) = -\left[\frac{(\kappa+\nu_\theta)\,\zeta^{-\kappa} + (\kappa-\nu_\theta)\,\zeta^{\kappa}}{2\,\kappa}\right]\left\{(1-\kappa^2)\,(1-\sqrt{\varepsilon}) - \hat{\omega}\,\rho_e^2\,\zeta^2\right\}\,. \tag{31}$$

Since both $\kappa + \nu_\theta$ and $\kappa - \nu_\theta$ are positive, $r'(\zeta) < 0$ for small ζ. For larger values of ζ, the sign of $r'(\zeta)$ depends on the sign of the expression inside the curly brackets. It follows from (31) that the only positive root of $r'(\zeta) = 0$ is given by

$$\zeta_1 = \sqrt{\frac{(1-\kappa^2)\,(1-\sqrt{\varepsilon})}{\hat{\omega}\,\rho_e^2}}\,. \tag{32}$$

Thus, provided that $\hat{p} < \hat{p}_0$, the function $r(\zeta)$ of (28) is positive at $\zeta = 0$ for $\hat{p} - \hat{q} \geq 0$, decreases for small values of ζ, has only one extremum for $\zeta \geq 0$, and is non-positive at $\zeta = 1$. Therefore, there exists a unique $\zeta \in [0, 1]$ that satisfies $r(\zeta) = 0$. Recall from Section 2 that $\hat{p} > \hat{q}$ yields $\varphi_\theta(\rho) < 0$ for the unconstrained disk problem.

If, however, $\hat{p} \geq \hat{p}_0$, we may have two, one, or, no roots of the algebraic equation (28), depending on the value of $r(\zeta_1)$, where ζ_1 is given by (32). To interpret these roots, we choose $\hat{p} = \hat{p}_0$ and increase $\hat{\omega}$ from zero. For $\hat{\omega} \leq (1-\kappa^2)\,(1-\sqrt{\varepsilon})$, we see from (32) that $\zeta_1 \geq 1$, which implies that $\zeta = 1$ is the only root of (28) in $[0, 1]$; therefore, $\det \nabla \mathbf{f} = \varepsilon$ in the entire disk. For $\hat{\omega} > (1-\kappa^2)\,(1-\sqrt{\varepsilon})$, we have that $\zeta_1 < 1$, which implies that (28) has two roots in $[0, 1]$.

The existence of two roots caused us to think that three, and not two, regions exist inside the disk. These are circular regions bounded by the radii ρ_a, ρ_b, and ρ_e, such that $(0, \rho_a)$, (ρ_a, ρ_b), and (ρ_b, ρ_e) are sub-intervals of $(0, \rho_e)$ where the constraint of local injectivity is active ($\det \nabla \mathbf{f} = \varepsilon$), non-active ($\det \nabla \mathbf{f} > \varepsilon$), and active, respectively. In this case, the first variation conditions for the existence of a minimizer $\mathbf{u}(\rho, \theta) = u(\rho)\,\mathbf{e}_\rho \in \mathcal{A}_\varepsilon$ of (19), (20) are similar to the equations (21)-(23) with the following modifications in the range of validity. The Euler-Lagrange equation (21.a) holds in both sub-intervals $(0, \rho_a)$ and (ρ_b, ρ_e). The other equation, (21.b), holds in (ρ_a, ρ_b). The jump conditions (23) hold across both $\rho = \rho_a$ and $\rho = \rho_b$. The kinematic and boundary conditions (22) remain the same. The procedure used to find the solution $(u, \hat{\lambda})$ of the corresponding equations is similar to the procedure used to find the solution $(u, \hat{\lambda})$ of the equations (21)-(23). The main difference is that now we have to solve two coupled algebraic equations, instead of only one, for the determination of both ρ_a and ρ_b. One of these equations is again obtained from the pressure condition (22.b) and the other equation is obtained from the continuity of traction across $\rho = \rho_b$. In Section 4 we find numerically up to four different roots $(\rho_a, \rho_b) \in [0, \rho_e] \times [0, \rho_e]$ for these equations, depending on the values of $\hat{p}$ and $\hat{\omega}$.

4. NUMERICAL RESULTS

We use the same numerical values considered by Fosdick & Royer-Carfagni (2001) for the geometric and material constants. Thus, the radius of the disk is $\rho_e = 1$, the elastic constants are $E_\rho = 99000$, $E_\theta = 990$, $\nu_\rho = 1$, $\nu_\theta = 0.01$, and the lower bound for the injectivity constraint is $\varepsilon = 0.1$. The applied load on the boundary of the disk, given by (11), is obtained from $\hat{p} = \hat{p}_0 + 0.1 = 0.79061$, where $\hat{p}_0$ is given by (30), and the angular velocity of the disk, given by (8.b), is obtained from $\hat{\omega} = (1-\kappa^2)\,(1-\sqrt{\varepsilon}) + 1 \cong 1.67693$. It then follows from (14) that $\hat{q} \cong 0.56147$. These values of $\hat{p}$ and $\hat{\omega}$ are large values in the context of Classical Linear Elasticity and are used here to show that three, and not two, non-intersecting regions may coexist inside the disk in the context of the constrained theory, which is nonlinear. Two of the three regions are such that $\det \nabla \mathbf{f} = \varepsilon$ and the third region is such that $\det \nabla \mathbf{f} > \varepsilon$.

First, however, we assume that two non-intersecting regions may coexist inside the disk so that $(0, \rho_e) = (0, \rho_a) \cup (\rho_a, \rho_e)$, where ρ_a is a root of the algebraic equation (28), and show that this assumption leads to $J \equiv \det(\mathbf{1} + \nabla \mathbf{u}) < \varepsilon$ in some sub-interval of $(0, \rho_e)$, which corresponds to a displacement field u that is not kinematically admissible, i.e., $u \notin \mathcal{A}_\varepsilon$, where $\mathcal{A}_\varepsilon$ is given by (18). Since $\hat{p} - \hat{q} > 0$, $\hat{p} - \hat{p}_0 > 0$, and $r(\zeta_1) = -0.06901$, where ζ_1 is given by (32) and is equal to 0.63535, it follows from Section 3 that the algebraic equation (28) has two roots, which are given by either $\rho_a \cong 0.36188$ or $\rho_a \cong 0.87492$. In the next two figures, we use these values of ρ_a to generate graphs for both J, given by (12), (24), (26), and (27), and $\hat{\lambda}$, given by (25) with $\tilde{\rho} = \rho_a$.

In Fig. 2 we show both J and $\hat{\lambda}$ plotted against the radius ρ for the root $\rho_a \cong 0.36188$. Observe from the graph on the left that J is equal to ε for $\rho \leq \rho_a$, is greater than ε in some intermediate region, and then becomes smaller than ε near $\rho = \rho_e$. Clearly, this is not acceptable and the corresponding solution u must be rejected. Nevertheless, observe from the graph on the right that $\hat{\lambda} \geq 0$ in $(0, \rho_a)$.

In Fig. 3 we show both J and $\hat{\lambda}$ plotted against the radius ρ for the root $\rho_a \cong 0.87492$. Observe from the figure on the left that $J = \varepsilon$ for $\rho \leq \rho_a$ and $J < \varepsilon$ for $\rho > \rho_a$. Again, this is not acceptable and the corresponding solution u must be rejected. Nevertheless, we see from the graph on the right that $\hat{\lambda} \geq 0$ in $(0, \rho_a)$. Thus, the assumption of only two coexisting regions does not lead to a kinematically admissible deformation.

Next, we consider that $(0, \rho_e) = (0, \rho_a) \cup (\rho_a, \rho_b) \cup (\rho_b, \rho_e)$, where both ρ_a and ρ_b are roots of the coupled algebraic equations discussed at the end of Section 3. To estimate the values of these roots, we square each of the two algebraic equations, sum the squares, and divide the resulting function by two. The zeroes of the corresponding quadratic function are the zeroes of the coupled algebraic equations. In Fig. 4 we show level curves of this quadratic function for $(\rho_a, \rho_b) \in$

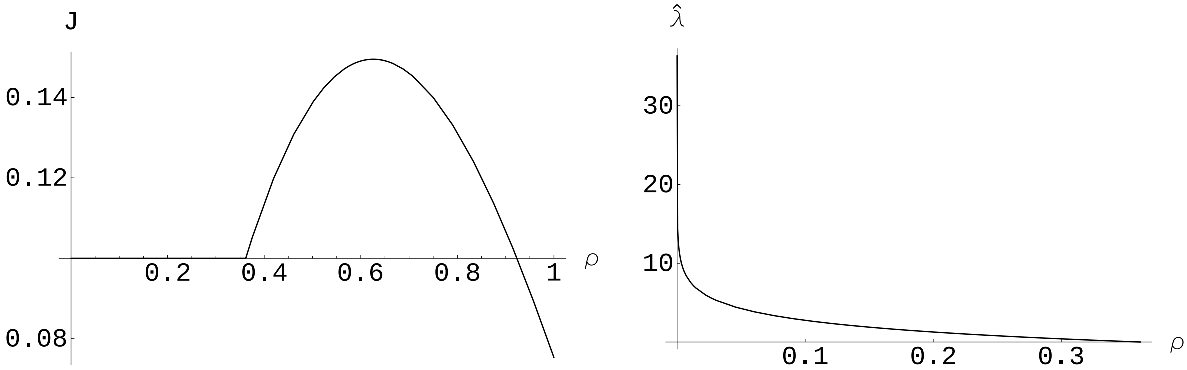

Figure 2. The Jacobian determinant J (left) and the multiplier $\hat{\lambda}$ (right) versus ρ for $\rho_a \cong 0.36188$.

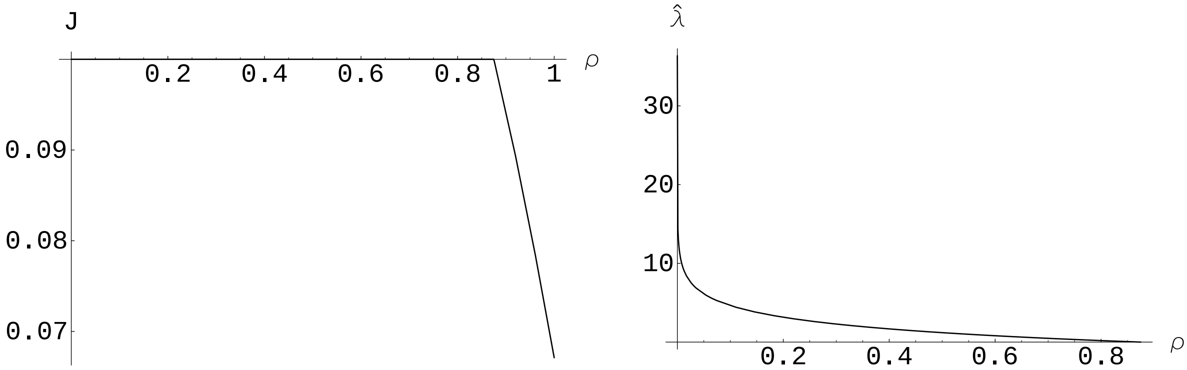

Figure 3. The Jacobian determinant J (left) and the multiplier $\hat{\lambda}$ (right) versus ρ for $\rho_a \cong 0.87492$.

$[0, \rho_e] \times [0, \rho_e]$. Observe from this figure that the quadratic function has four points of extremum. We computed these points and found that they are roots of the coupled algebraic equations. The points are $(\rho_a^{(1)}, \rho_b^{(1)}) \cong (0.41638, 0.41638)$, $(\rho_a^{(2)}, \rho_b^{(2)}) \cong (0.35788, 0.92748)$, $(\rho_a^{(3)}, \rho_b^{(3)}) \cong (0.84935, 0.47376)$, and $(\rho_a^{(4)}, \rho_b^{(4)}) \cong (0.88369, 0.88369)$.

We have verified that the only point that generates a kinematically admissible solution $\hat{u}$ with $\hat{\lambda} \geq 0$ in $(0, \rho_e)$ is the second one. Notice that this point is the closest to the point $(0.36188, 0.87492)$, which was presented above by considering only two regions. Below we show figures of J and $\hat{\lambda}$ considering the roots $(\rho_a, \rho_b) \cong (0.35788, 0.92748)$.

In Fig. 5 we show J versus ρ. Observe from the graph that J is equal to ε for $\rho \leq \rho_a$, is greater than ε in some intermediate region, and is equal to ε for $\rho \geq \rho_b$.

In Fig. 6 we show $\hat{\lambda}$ versus ρ. The graph on the left corresponds to $\hat{\lambda}$ versus ρ in the interval $(0, \rho_a)$ and the graph on the right corresponds to $\hat{\lambda}$ versus ρ in the interval (ρ_b, ρ_e). Observe from both graphs that $\hat{\lambda} \geq 0$ in the corresponding intervals.

In addition to the calculations above, we have used the numerical procedure described in Aguiar (2006), which is based on an Interior Penalty Formulation of the minimization problem (19)-(20), to compute an approximate solution for the rotating disk problem under external pressure. Here, no *a priori* assumptions are made about the number of coexistent regions. In Fig. 7 we show the numerical approximation of J, obtained with a Finite Element mesh of 500 linear elements and represented by the dash-dotted line, plotted against the radius ρ. Observe that the corresponding curve is very similar to the curve shown in Fig. 5. For comparison purposes, we also show J calculated from the expressions (12), (24), (26), and (27), which corresponds to the case of two coexistent regions. The corresponding curve is represented by the solid line and is the same curve shown in the graph on the left of Fig. 2. Notice from Fig. 7 that both lines are close to each other for $\rho \in (0, \rho_b^{(2)})$, where we recall from above that $\rho_b^{(2)} = 0.92748$.

5. ACKNOWLEDGEMENTS

The authors wish to acknowledge FAPESP (Fundacão de Amparo à Pesquisa do Estado de São Paulo), proc. # 2006/50009-0 R, and the University of Minnesota Supercomputing Institute for Digital Simulation and Advanced Com-

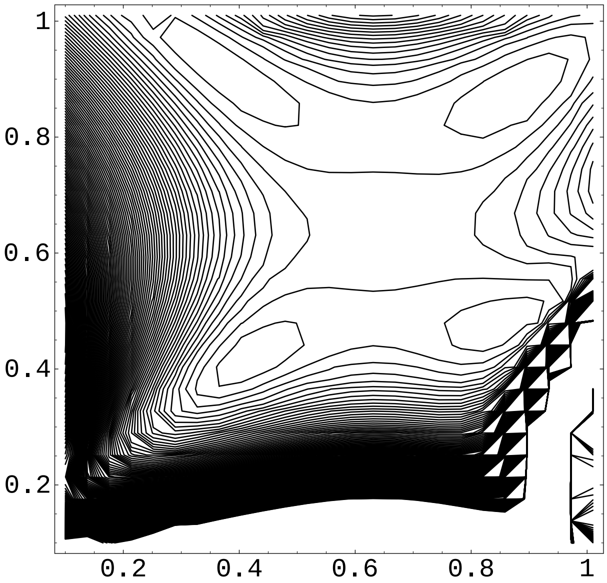

Figure 4. Level curves to estimate the roots of coupled algebraic equations.

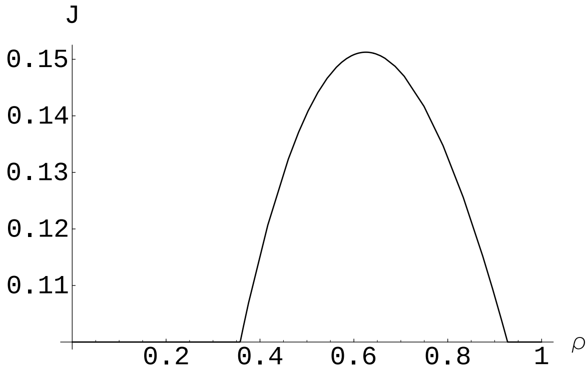

Figure 5. The Jacobian determinant J versus ρ for $(\rho_a, \rho_b) \cong (0.35788, 0.92748)$.

putation for their support of this research.

APPENDIX A

Proposition: To be consistent with $\hat{\lambda}(\rho) \geq 0$ in $(0, \rho_a)$, the jump of u' across $\rho = \rho_a$ must be zero and $\tilde{\rho} = \rho_a$.

Proof. We use an analogous procedure considered by Fosdick & Royer-Carfagni (2001) in the analysis of a model problem that is a particular case of our problem when $\hat{\omega} = 0$.

First, we substitute the expressions (24) and (25) in the jump condition (23.b) to obtain

$$-(1-\kappa^2)\,(1-\sqrt{\varepsilon})\,\log\left(\frac{\rho_a}{\tilde{\rho}}\right) = -|[u'(\rho_a)]| - \frac{\hat{\omega}}{2}\left[\rho_a^2 - \tilde{\rho}^2\right], \tag{33}$$

where $|[u'(\rho_a)]| \equiv u'(\rho_a^+) - u'(\rho_a^-)$ is the jump of u' across $\rho = \rho_a$.

Noting that $\log(\rho/\tilde{\rho}) = \log(\rho/\rho_a) + \log(\rho_a/\tilde{\rho})$ and using (33) in (25), we can rewrite $\hat{\lambda}$ as

$$\hat{\lambda}(\rho) = \frac{1}{\sqrt{\varepsilon}}\left[\frac{\hat{\omega}}{2}\left[\rho^2 - \rho_a^2\right] - (1-\kappa^2)\,(1-\sqrt{\varepsilon})\log\left(\frac{\rho}{\rho_a}\right)\right] - \frac{1}{\sqrt{\varepsilon}}|[u'(\rho_a)]|\,. \tag{34}$$

Since $\lambda(\rho_a) \geq 0$, we see from (34) that $|[u'(\rho_a)]| \leq 0$, which implies that

$$u'(\rho_a^+) \leq u'(\rho_a^-)\,. \tag{35}$$

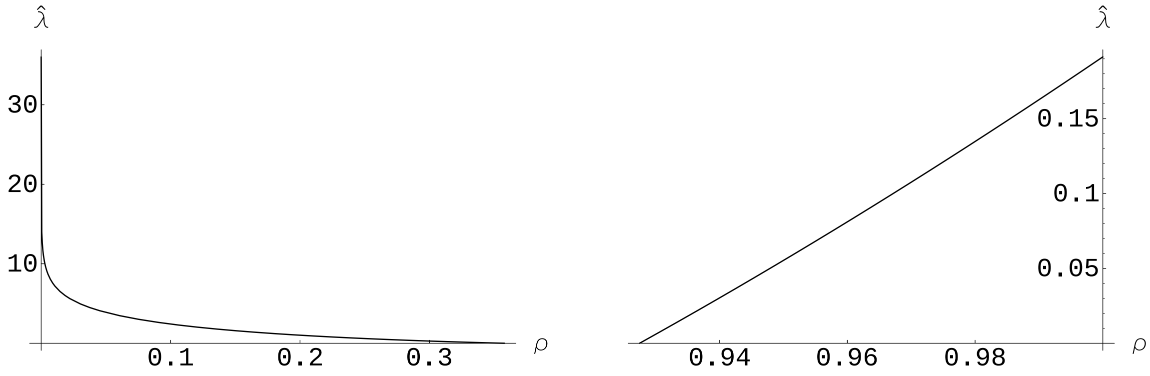

Figure 6. The multiplier $\hat{\lambda}$ versus ρ for $(\rho_a, \rho_b) \cong (0.35788, 0.92748)$.

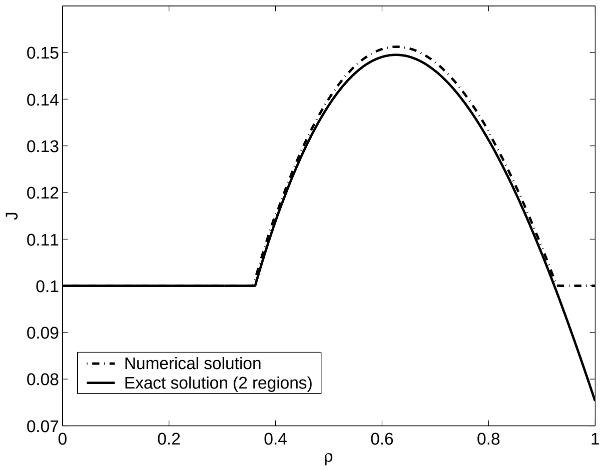

Figure 7. The Jacobian determinant J versus ρ.

On the other hand, the condition $\det \nabla \mathbf{f} \geq \varepsilon$ together with (12) lead to $(1 + u'(\rho_a^+))\,(1 + u(\rho_a^+)/\rho_a) \geq \varepsilon$, where $u(\rho_a^+) = u(\rho_a^-)$ from the jump condition (23.a). Since $\det \nabla \mathbf{f} = (1 + u'(\rho))\,(1 + u(\rho)/\rho) = \varepsilon$ for $\rho \in (0, \rho_a)$, we then find that

$$u'(\rho_a^+) \geq u'(\rho_a^-)\,. \tag{36}$$

Next, we observe from both (25) and (34) that $\hat{\lambda}$ is a convex function of ρ in the interval $(0, \rho_a)$ and vanishes at both $\tilde{\rho}$ and ρ_a. Since $\hat{\lambda}(\rho) \geq 0$ for $\rho \in (0, \rho_a)$, we find that $\tilde{\rho} = \rho_a$.

6. REFERENCES

Aguiar, A. R. and Fosdick, R. L., 2001, "Self-intersection in elasticity". *Int. J. Solids Structures* **38**, 4797–4823.

Aguiar, A. R., 2006, "Local and Global Injective Solution of the Rotationally Symmetric Sphere Problem". *Journal of Elasticity* **84**, 99–129.

Fosdick, R. L. and Royer-Carfagni, G., 2001, "The constraint of local injectivity in linear elasticity theory". *Proc. R. Soc. Lond. A* **457**, 2167–2187.

Gurtin, M. E., 1981, "An Introduction to Continuum Mechanics". London: Academic Press Inc..

Lekhnitskii, S. G., 1968, "Anisotropic Plates". New York: Gordon and Breach Science Publishers.

Obeidat, K., Stolarski, H., Fosdick, R., and Royer-Carfagni, G., 2001, "Numerical analysis of elastic problems with injectivity constraints". In *European Conference on Computational Mechanics (ECCM-2001)*.

7. Responsibility notice

The authors are the only responsible for the printed material included in this paper.